

Development of a MicroStrip Gas Chamber as a Time-Resolved Area Detector

Toru Tanimori,* Shunsuke Aoki, Yuji Nishi and Atsuhiko Ochi

Department of Physics, Tokyo Institute of Technology, Tokyo 152, Japan.

E-mail: tanimori@hp.phys.titech.ac.jp

(Received 4 August 1997; accepted 12 January 1998)

A two-dimensional microstrip gas chamber (MSGC) has been developed with a 10 cm-square detection area and an ultrafast read-out system. The MSGC was made using multi-chip module (MCM) technology, and has a very thin substrate of 17 μm and many anodes and back strips, both with 200 μm pitches. The new read-out system, in which the hit addresses of the electrodes were sequentially encoded to the hit positions by a synchronous clock, handles data rates of up to 10^7 events s^{-1} from MSGCs. This enables the acquisition of fast and sequential digital images. Furthermore, since the MSGC is a real photon-counting detector, the timing of the photons, to an accuracy of a few tens of nanoseconds, and energy can be recorded. Here, the performance of the MSGC system as a real-time area detector is reported, and the abilities of this system are discussed.

Keywords: microstrip gas chambers (MSGCs); area detectors; time-resolved studies.

1. Introduction

The microstrip gas chamber (MSGC) was proposed in 1988 by Oed (1988) as a new type of proportional gas detector providing excellent position resolution. It is known that this new detector would satisfy almost all of the requirements for a tracking detector in the next decade: (i) stable operation under a high luminosity condition, (ii) a good position resolution of about a few tens of micrometres, (iii) radiation hardness and aging resistivity. These are also important requirements for imaging X-ray detectors operated in a high-intensity radiation environment.

An MSGC is generally produced using microelectronics technology, by which sequences of alternating thin anodes and cathodes are formed with a few hundred micrometres pitch on an insulating substrate. The closeness of the electrodes and the simplicity of the structure are regarded as the key factors in fulfilling these requirements. Whereas most MSGCs have so far been realized on glass or quartz substrates, for several years we have been developing another type of MSGC having a ~ 10 μm thin polyimide substrate (Nagae *et al.*, 1992; Tanimori *et al.*, 1996). Our MSGC is made using multi-chip module (MCM) technology, which allows a high-density assembly of bare silicon large-scale integration (LSI) chips on a silicon or ceramic board. This technology has been generally available from semiconductor companies, and makes it possible to use various kinds of microelectronics technology such as through-hole, formation of a micro-register or capacitor, and so on. All of our MSGCs are made in collaboration with the PCV and Module Division of Toshiba Co. Ltd.

Polyimide can be easily made into a very extensive and uniform substrate having a perfectly flat and smooth surface due to its softness and elasticity. In addition, polyimide can be formed into any desired shape on the micrometre scale by MCM technology; in our MSGC, guarding masks on cathodes and through-holes are formed by this technique.

A very thin substrate of our MSGC enables us to control the flow of positive ions from anodes to cathodes by optimizing the potential on the backplane. Also, because of the thickness of only a few micrometres between the backplane and anode, a fast signal is induced on the backplane enabling two-dimensional readout from one MSGC. The basic operational properties of our specific MSGC were studied by Nagae *et al.* (1992) and Tanimori *et al.* (1992). From those studies, a 5 cm-square two-dimensional MSGC with 200 μm anode and back-strip pitches was made as a second step. The read-out system was developed to handle ~ 500 channels of this MSGC for obtaining two-dimensional X-ray images, using the conventional techniques of high-energy physics. The features of the MSGC area detector have been described recently in detail by Tanimori *et al.* (1996), who examined position resolution, stability, durability and operation under high counting rates. In this study the large potential of the MSGC as an X-ray area detector was verified.

However, there still remain critical problems to be overcome for the applications of imaging MSGCs: for example, how to handle the huge quantity of data from the MSGC in the real-time image processing. Recently, we developed a new type of readout system in which the data are synchronously managed by digital electronics. Using

this new system, we were able to obtain real-time movies from the MSGC. In addition, we examined new ideas of X-ray imaging analyses using the unique features of the MSGC. Here we report on these new outcomes from our recent study of the MSGC.

2. Two-dimensional MSGC

Fig. 1 shows a schematic diagram of our two-dimensional MSGC, which is formed on a $20\ \mu\text{m}$ thin polyimide substrate. On the polyimide layer, $10\ \mu\text{m}$ -wide anodes and $100\ \mu\text{m}$ -wide cathodes are formed by photolithography technology. Between the ceramic base and the polyimide substrate, there are back strips with a $200\ \mu\text{m}$ pitch orthogonal to the anode, which provide information in the second dimension. All electrodes are made of gold with a thickness of $1\ \mu\text{m}$. In order to reduce the effect of parallax broadening of the position distributions, a drift plane is placed $3\ \text{mm}$ above the substrate. Every 15 (32) cathode strips are aggregated to form one group at one end of the $5\ \text{cm}$ -square ($10\ \text{cm}$ -square) MSGC; there are 17 cathode groups to which high voltages are independently supplied. The signal from groups of cathodes can conveniently be used as an energy measurement of an X-ray. The edge of the cathode is coated with polyimide with a width of $\sim 7\ \mu\text{m}$ for suppressing discharges between anodes and cathodes. This coating effectively suppresses the discharge from the cathode edge, and drastically increases the durability against dust attached to the surface (Tanimori *et al.*, 1996). The back strips are connected to the ground. A gas mixture of Ar (50%) and C_2H_6 (50%) was used under

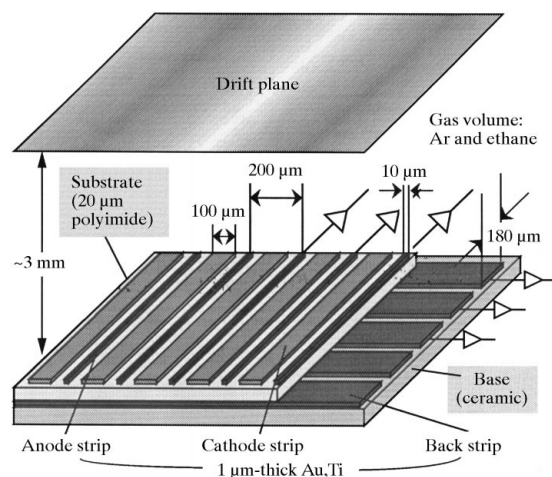


Figure 1

Schematic structure of the two-dimensional MSGC which was formed on a $17\ \mu\text{m}$ thin polyimide substrate. On the polyimide layer, $7\ \mu\text{m}$ -wide anodes and $63\ \mu\text{m}$ -wide cathodes were formed with a $200\ \mu\text{m}$ pitch (the width of the cathodes was changed to $100\ \mu\text{m}$ in the imaging measurement as mentioned in §4). Between the ceramic base and the polyimide substrate are set back strips with a $200\ \mu\text{m}$ pitch orthogonal to the anodes. All electrodes are made of gold with a thickness of $1\ \mu\text{m}$. To define the drift field, the drift plane was placed at $10\ \text{mm}$ above the substrate.

atmospheric pressure. The absorption efficiency under these conditions (*i.e.* a $3\ \text{mm}$ gap and the use of the above gas) is $\sim 4\%$ for $8.9\ \text{keV}$ X-rays. The use of pressured Xe gas will be necessary to obtain the sufficient absorption efficiency of $\sim 30\%$ in the near future.

In an MSGC the resistivity of the substrate is considered to be a key factor for maintaining stable operation under a high counting rate. We used an organic titanium coating on the surface of polyimide of very small thickness, from which a surface resistivity of $\sim 10^{15}\ \Omega\ \text{square}^{-1}$ was obtained. We found an optimum operating point by adjusting both the thickness of the substrate and the potential of both anodes and cathodes. Details of the gas-amplification features and stability of the MSGC are reported by Tanimori *et al.* (1996).

3. Read-out electronics system

For a quick evaluation of the newly developed MSGC, a $5\ \text{cm}$ -square MSGC package was developed, in which the MSGC sits on a large pin grid array (PGA) package having more than 500 pins on the reverse side, as shown in Fig. 2 (Tanimori *et al.*, 1996). The new $10\ \text{cm}$ -square MSGC was directly mounted onto the $30\ \text{cm}$ -square mother board by a bonding technique to reduce the space of the mother board. In addition, various ideas were adopted for the mother board to handle more than a thousand signals in a $30\ \text{cm}$ -square size, *i.e.* an eight-layer structure and the micro-register arrays attached by bonding. Fig. 3 shows the mother board and the gas vessel in which the $10\ \text{cm}$ -square MSGC is mounted. The pre-amplifier cards are inserted vertically into the connector on the rear side of the mother board, which has 64 fast amplifiers (MQS104 developed by LeCroy) and discriminators. All discriminated signals from the anodes and cathodes (ECL level) are fed to the newly developed position-encoded system.

Fig. 4 shows digital oscilloscope images of output signals of one anode generated from an MQS04 fast amplifier at counting rates of a few megahertz per anode. Each pulse width is $\sim 30\ \text{ns}$ and is clearly distinguished. This is a very

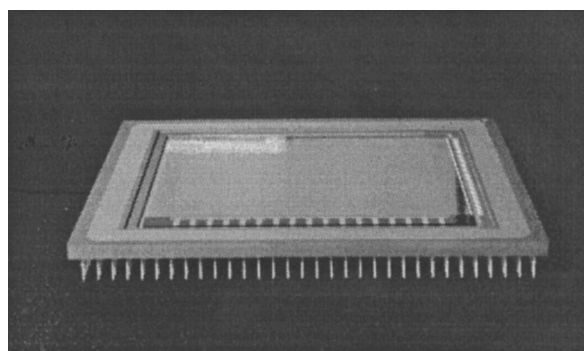


Figure 2

Photograph of the MSGC package on which a $5\ \text{cm}$ -square two-dimensional MSGC was mounted. The package is made of ceramics with an $8\ \text{cm}$ -square size, and has 541 pins with a $0.1\ \text{inch}$ pitch on the reverse side.

important point to keep in mind when considering how to derive the coordinates of the X-ray under such a high counting rate. As pointed out by Tanimori *et al.* (1996) concerning the 5 cm-square MSGC, the fast and narrow pulses of both anodes and back strips provide a very sharp timing coincidence between the anodes and back strips, within ~ 10 ns. This means that the two coordinates of a hit point are able to be synchronously encoded from the MSGC within a few tens of nanoseconds by requiring coincidence in the timings of both anodes and back strips. This procedure enables us to encode more than 10^7 events s^{-1} , which is ten times superior to the ability of the conventional delay-line method. This procedure appears to be insufficient for making the most of the capability of MSGCs. However, the MSGC continuously generates data of a few tens of megabytes when operating at ~ 10 MHz, in which the transfer rate from the MSGC to the computer reaches a limit manageable by present computer technology.

Most of the events produce less than three hits on both anodes and back strips. The simple method of making the

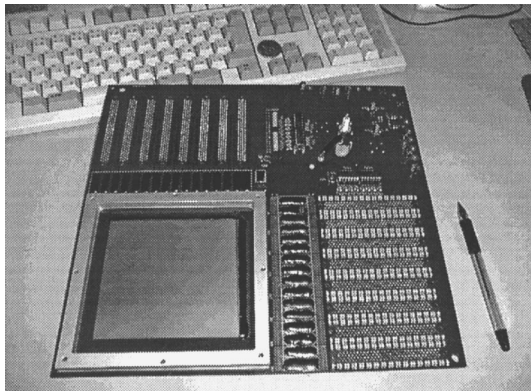


Figure 3
Top view of a new 10 cm-square-MSGC mother board. The MSGC is mounted in the gas vessel seen on the lower right of the mother board.

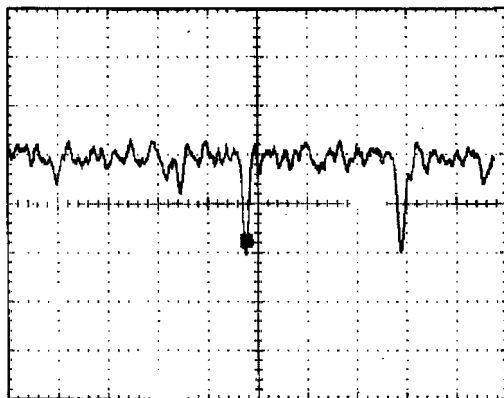


Figure 4
Digital oscilloscope image of output signals from one anode at counting rates of ~ 10 MHz per anode. Each pulse is clearly distinguished even at such a high counting rate.

hit position the centre of gravity of the hit electrodes was proved to provide a position resolution of less than $100 \mu m$, as shown by Tanimori *et al.* (1996). This resolution reaches a limit due to the diffusion of drift electrons. Therefore, we need to record only the positions of the hit anodes and back strips instead of the pulse heights of those electrodes.

We have developed a synchronous encoding system based on the above strategy. This system consists of 9-U VME modules of two types. One is the position-encoding module (PEM) which has 128 inputs and trees of programmable logic devices (PLD); the PEM encodes hit strips to X or Y coordinates. The other is the control and memory module (CMM) which has a large buffer memory of ~ 200 Mbyte for keeping the image data for ~ 10 s at a counting rate of 10^7 events s^{-1} , and generates the synchronous clock. A block diagram of the new read-out system and photographs are shown in Figs. 5 and 6, respectively.

In the PEM, at first, asynchronous input signals from anodes and back strips are modulated to synchronous ones with the internal clock of ~ 20 MHz sent from the CMM. Secondly, the positions of the hit electrodes are synchronously encoded in trees of PLD, in which only one cluster of sequential hit electrodes are encoded; two more clusters are rejected here. Also, in this stage both hits on anodes and back strips are required within the same clock cycle to avoid electrical noise. The arithmetic centroid and the number of electrodes in the cluster are calculated in PLD and transferred to the CMM. All functions in PLD are synchronized. In the case of the 10 cm-square MSGC, four PEMs for X and Y coordinates and one CMM are needed, all of which communicate using a J3 VME bus. The data in the memory buffer of the CMM were transferred to the CPU in the same VME crate using a J1 VME bus. In this

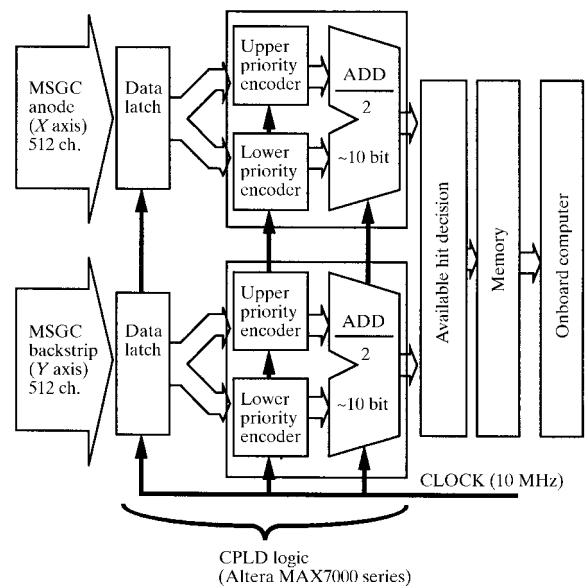
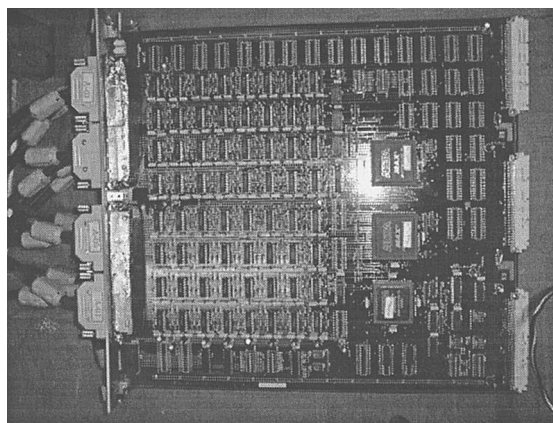


Figure 5
Block diagram of the new synchronous read-out system.

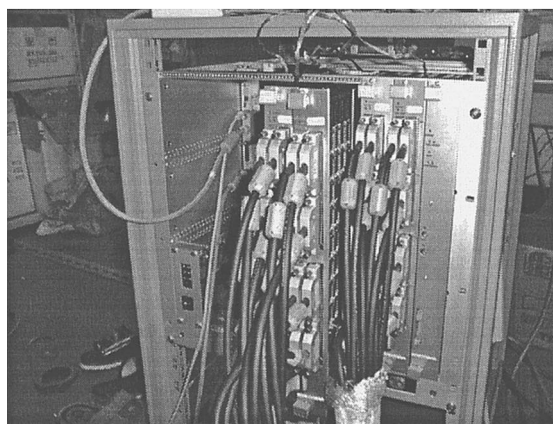
CPU, data were recorded on the hard disk or transferred to another workstation *via* a fast network. The power of the CPU and transfer speed to the hard disk restricts the performance of the MSGC for compiling images. A recently developed 64-bit CPU enables one to picture real-time movies, but such high-performance CPUs are still not available in the VME on-board type. In our new system, a few frames per second can be drawn in real time using the VME CPU (110 MHz microSparc).

Fig. 7 shows the performances of the data handling for both the CAMAC system described by Tanimori *et al.* (1996) and the new system. The new system can handle 3 MHz events, which is more than 3×10^3 times the ability of the CAMAC system. This enables us to take ~ 30 frames s^{-1} of images of high enough quality. Figs. 8(a) and 8(b) show the images of the small metal pendant obtained from the CAMAC system and the new system during 1 s, which clearly indicate the ability of the new system. Here we present X-ray movies of the rotating metal small pendant taken by the new read-out system.

Details of the new read-out system are described by Ochi *et al.* (1998).



(a)



(b)

Figure 6

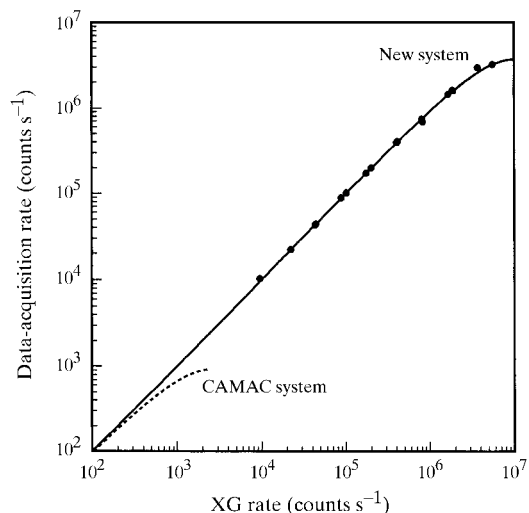
Photographs of (a) the side view of the PEMS in which three PLDs, the main part of this module, occupy only one-fifth on the right. The ICs on the left are ECL-TTL transfers. (b) View of the PEMS and the CMM inserted into the 9U VME crate.

4. Imaging performance

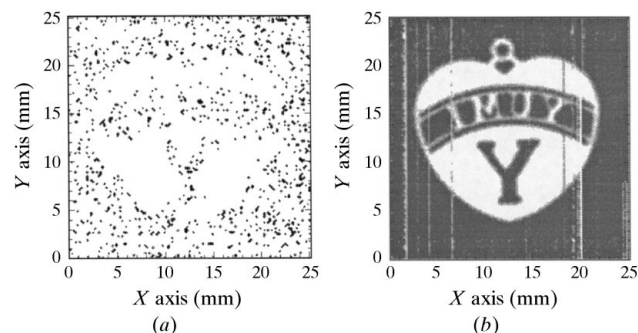
A good example of an X-ray image obtained from the MSGC is presented in Fig. 9. This is a transmission image of the circuit board having very fine through-holes with a 300 μm diameter and a 600 μm pitch in line. Each through-hole is separated from the other. Furthermore, note that the printed pattern on the circuit board can also be seen, which indicates that the digital image of X-rays in the MSGC allows us to measure the small variations of material density.

Recently, an X-ray beam test for the 5 cm-square MSGC was carried out at the Photon Factory at KEK to verify the X-ray imaging ability. Measurements were performed on beamline 6C in December 1996.

Fig. 10(a) shows a small-angle diffraction pattern of the collagen irradiated by an 8.9 keV X-ray beam of 1 mm-square size. Fig. 10(b) is a projected plot along the axis normal to the beam. Note that both the large peaks and small peaks appear very symmetrically from the beam position, which is an excellent feature of both the fine electrode pitch of the MSGC and the wide dynamic range

**Figure 7**

Comparison of the data-handling performances for the CAMAC system and our synchronous read-out system.

**Figure 8**

Transmission images of a small metal pendant obtained with the MSGC during 1 s measurement, using (a) the CAMAC system and (b) the new system.

of the photon counting, although peak widths were determined not from the position resolution of the MSGC but from the beam size of 1 mm. Furthermore, very small peaks around the tail of the large peaks can be clearly distinguished, which shows that the spread function of the MSGC has no halo around diffraction peaks as mentioned by Tanimori *et al.* (1996).

We report on a new approach to the Weissenberg camera using the timing information of the X-rays. Fig. 11 shows the X-ray diffraction image of a crystal of phenothiazine–benzolic acid complex based on an oscillation method and Weissenberg camera, in which the sample crystal at 10 cm in front of the MSGC was rotated continuously around an axis normal to the incident 8.9 keV monochromatic X-ray beam of 1 mm-square size.

In general, a two-dimensional image of a diffraction pattern is not sufficient for obtaining three-dimensional information of the objective crystal. When using a monochromatic X-ray beam, several diffraction patterns are taken varying the angle between one axis of the crystal and the X-ray beam over an acceptable angle range. The MSGC can record the arriving time of each X-ray photon with a few tens of nanoseconds resolution. The timing just gives us information on the angle of rotation of the crystal with a fine angular resolution. This allows us to obtain all the information needed for three-dimensional crystal analysis from only one measurement.

The projection of Fig. 11 onto the X coordinate is shown in Fig. 12(a), where many diffraction peaks and a contin-

uous background are seen. The angle information for each diffraction peak are not seen in this figure. For one small angle, shown by the arrows in this figure, the plot of events in this peak *versus* the phase coordinate is presented in Fig. 12(b).

A clear peak concentrated over 2° is found, which indicates that the noise away from the peak can be removed easily using the angle information. Fig. 12(c) shows Fig. 12(a) after applying this noise-reduction method. There remains very little noise below the clear peak. Using this method, the sensitivity can be improved more than ten times.

Laue diffraction patterns are commonly used for studying crystals, generally for the determination of the structure of unknown crystals. In order to reconstruct the structure of the crystal from the two-dimensional pattern, information about the other dimension is necessary. The third-dimension information appears as an energy of each diffraction peak, in the Laue pattern, which is taken using a white X-ray beam. In this measurement, the counting rate was very high, which caused a pile-up problem for pulses fed to the ADC. The energy resolution of X-rays was then too poor to sufficiently distinguish the energy of the diffraction peaks. We are now developing an ADC

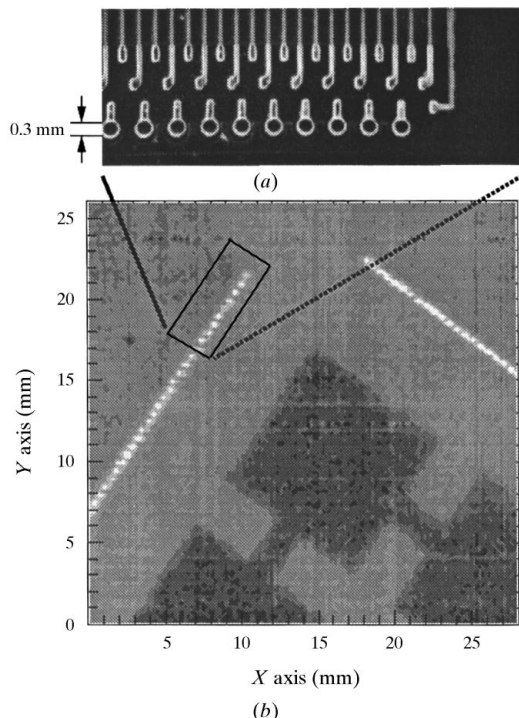


Figure 9

Transmission image for the printed board in which very fine through-holes of 300 μm diameter and 600 μm pitch (a) are formed in a line, and can be seen (b).

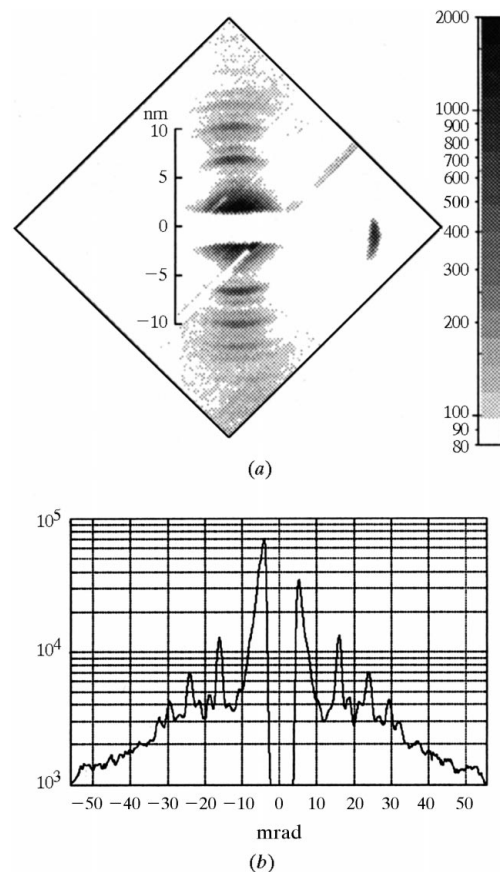


Figure 10

(a) Small-angle diffraction pattern of the collagen irradiated by a 10 keV X-ray beam with a 0.5 mm-square size. (b) Projected plot of (a) to the axis normal to the beam.

system having a similar structure to that of a flash ADC to operate at high counting rates.

Finally we discuss the ultimate time-resolved image for the periodic variation or reaction. An imaging device based on the photon-counting method, such as MWPC or MSGC, has an essential upper limit of $\leq 10^7$ events s^{-1} for handling the data, which restricts the number of picture frames to less than $100 s^{-1}$. However, fast processes with variation times of microseconds can be observed as continuous images if periodic measurements are performed for this process. Since the MSGC records both the timing of each detected X-ray and the start of each periodic process, all X-rays recorded by the MSGC can be folded into one phase of the periodic process. When a process with a variation time of $100 \mu s$ is measured periodically by the MSGC at an event rate of 10 MHz for 10 s, hundreds of images with $\sim 1 \mu s$ timing bin could be obtained in one process. Each image, made of about 10^6 X-rays, gives a high-quality picture. The shortest timing bin of one image is determined by the system clock of 20 MHz and the Poisson accidental distribution, and estimated to be 100 ns.

5. Summary and perspective

We have developed a two-dimensional MSGC and a fast read-out electronics system, both of which are essential developments to realize a new time-resolved X-ray area detector. Since the MSGC is a differential-type detector, the MSGC area detector can provide not only the digital time-resolved image with fine position resolution and a large dynamic range, but also a fairly new type of image including other information such as fine-timing (phase) and energy as mentioned above. These new types of images will provide a new approach in X-ray imaging analysis.

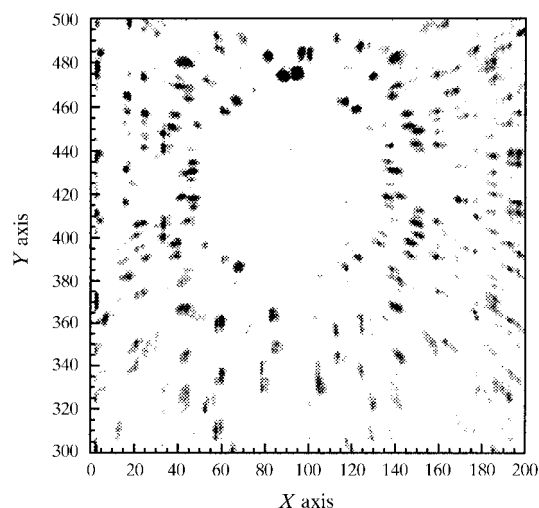


Figure 11

X-ray diffraction image of the phenothiazine-benzilic acid complex in which the sample crystal at 10 cm in front of the MSGC was rotated continuously along the axis normal to the incident monochromatic X-ray beam.

In addition, we stress that this detector system is a completely electric system controlled by computer, where electric system means not only that the data are completely electrically transferred to computers, but also that all the components of the MSGC system are made from integrated circuit (IC) or LSI technology. The MSGC itself is made using high-density printed-board technology for the direct mounting of a bare LSI. All electrical elements of the MSGC read-out system are made of commercially available LSI chips. Fast amplifiers and comparators attached to the MSGC amp-card (MQS104 and MVL407 of LeCroy, respectively, both 4 channels in one chip), and the ECL-TTL transfer chips in the PEMs are the main elements of the read-out system. The PLDs, the core parts of the read-out system, occupy less than 10% of the system.

As a next step to the improvement of the MSGC, we intend to change both the amplifier and the discriminator to higher-density ICs having 32 channels in one chip which can be mounted directly on the MSGC mother board. PLDs for position encoding may also be set in the MSGC box, and no ECL-TTL transfer chip is needed. This improvement will realize a thin MSGC imager similar to a liquid-crystal display in the near future. These improvements can be made using the available technologies.

However, there still remains one crucial problem which may prevent MSGCs from stable operation: discharges damage the electrodes of an MSGC. The discharge process in MSGCs has been studied in detail by Peskov *et al.* (1996). Although we do not yet know the complete diagnosis of discharges in an MSGC, the tolerance can be increased by a combination of improvements. About 5–8%

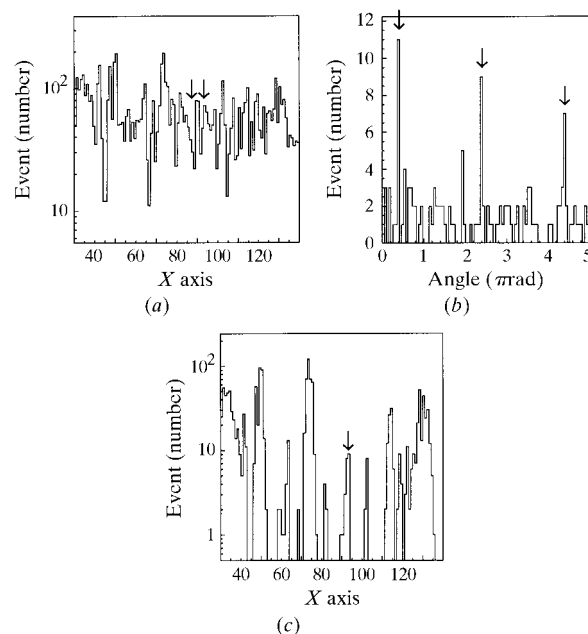


Figure 12

(a) Projection of Fig. 11 onto the X coordinate. (b) Event plot via the phase coordinate for the peak located between two arrows in (a). (c) Same as (a) after applying this noise-reduction method.

of electrodes were damaged by discharges during a one-year operation in our experience, testing many 5 cm-square MSGCs. Since damage due to discharges usually concentrated in warming up at the first use, dust and parts of poor-quality electrodes might be the reasons for discharges.

We are now studying the following in order to suppress discharges between anodes and cathodes: (i) cleanliness of the surface and the electrode, (ii) electrode material (higher melting point), (iii) gas mixture, (iv) electrode shape and its passivation (see Tanimori *et al.*, 1996), and (v) improvement of the quality of manufacturing. Another solution is the insertion of an intermediate gas multiplier such as GEM proposed by Bouclier *et al.* (1997). We are also investigating the capillary plate as an intermediate gas multiplier the gain of which is expected to be ~20–30. Gas multiplication in a capillary plate has already been confirmed by Sakurai *et al.* (1996). Capillary plates up to ~10 cm in diameter are commercially available. Therefore, capillary plates will soon be used in the 10 cm-square MSGC, if it operates well with the 5 cm-square MSGC.

Although we are not stating that the technology of an MSGC has been established, it is very clear that the MSGC will provide a new innovative approach to imaging analysis methods using X-rays, charged particles and neutrons.

The authors would like to thank Dr T. Ueki, Dr M. Suzuki, Dr T. Fujisawa, Dr Toyokawa and members of the

Biological Physics group of The Institute of Physical and Chemical Research (RIKEN) for continuous support and encouragement. We gratefully acknowledge the kind support and fruitful discussion of Professor Y. Ohashi, Dr H. Uekusa and their colleagues of the Department of Chemistry, Tokyo Institute of Technology. We also thank the staff of the Photon factory at KEK. This work is supported by RIKEN, CREST, Japan Science and Technology Corporation (JST), and a Grant-in-Aid of Scientific Research of the Japan Ministry of Education, Science, Sports and Culture.

References

- Bouclier, R., Dominik, W., Hoch, M., Labbe, J. C., Million, G., Ropelewski, L., Sauli, F., Sharma, A. & Manzin, G. (1997). *Nucl. Instrum. Methods*, **A396**, 50–66.
- Nagae, T., Tanimori, T., Kobayashi, T. & Miyagi, T. (1992). *Nucl. Instrum. Methods*, **A323**, 236–239.
- Ochi, A., Tanimori, T., Nishi, Y., Aoki, S. & Nishi, Y. (1998). *J. Synchrotron Rad.* **5**, 1119–1122.
- Oed, A. (1988). *Nucl. Instrum. Methods*, **A263**, 351.
- Peskov, V., Ramsey, B. D. & Fonte, P. (1996). MSFC/NASA preprint LIP/96–11.
- Sakurai, H., Tamura, T., Gunji, S. & Noma, M. (1996). *Nucl. Instrum. Methods*, **A374**, 341–344.
- Tanimori, T., Minami, S., Nagae, T., Takahashi, T. & Miyagi, T. (1992). *Proc. SPIE*, **1734**, 68–77.
- Tanimori, T., Ochi, A., Minami, S. & Nagae, T. (1996). *Nucl. Instrum. Methods*, **A381**, 280–288.